Relaxation process from photoinduced states of double-step spin-crossover systems using a kinetic two-sublattice Ising-like model including intra-site coupling

Shinichiro Mouri* and Koichiro Tanaka†
Department of Physics, Kyoto University, Kitashirakawa Oiwaketyo, Sakyo-ku, Kyoto 606-8502, Japan

Sébastien Bonhommeau
Laboratoire de Chimie de Coordination (LCC/CNRS/UPR8241), Centre National de la Recherche Scientifique, 205, Route de Narbonne, 31077 Toulouse, France
and Laboratoire de Physique des Solides de Toulouse, UMR 5477 CNRS, 118 Route de Narbonne, F-31062 Toulouse Cedex, France

Nawel Ould Moussa, Gábor Molnár, and Azzedine Bousseksou‡
Laboratoire de Chimie de Coordination (LCC/CNRS/UPR8241), Centre National de la Recherche Scientifique, 205, Route de Narbonne, 31077 Toulouse, France

(Received 7 September 2007; revised manuscript received 24 September 2008; published 18 November 2008)

A two-sublattice kinetic mean-field Ising-like model is proposed to describe the relaxation process from photo-induced metastable states in double-step spin-crossover complexes. Its originality lies in the rigorous treatment of intra-site coupling that yields dynamical equations by using additionally the Glauber stochastic treatment of master equations. The numerical resolution of these equations permits one to extract not only the high-spin fraction but also the intra-site correlation and the symmetry-breaking parameter which are hidden order parameters in these systems. Our simulation can demonstrate interesting relaxation behavior. As the result of synergy of inter- and intra-site interactions, double-step relaxation curves can be obtained in most cases. When decreasing the magnitude of interactions, one-step sigmoidal relaxation or stretched exponential relaxations appear. Asymmetry between *A* and *B* sublattices may even induce curious dynamics such as triple steplike behavior that is also observed for weak fluctuations in the initial configuration. For stronger fluctuations the system relaxes to an ordered metastable state instead of reaching the ground state. This model is finally applied to genuine systems, namely, the binuclear spin-crossover complex $[Fe(bt)(NCS)_2]_2(bpym)$ and the polymeric spin-crossover compound $\{Fe(pmd)[Ag(CN)_2]Ag_2(CN)_3\}$ that exhibit both a two steps thermal spin transition. The relaxation curves are then conveniently reproduced considering weak-interaction parameters whose possible origins will be highlighted.

DOI: 10.1103/PhysRevB.78.174308 PACS number(s): 75.30.Wx, 64.60.My

I. INTRODUCTION

Photo-induced phase transitions (PIPT) (Refs. 1 and 2) are highly cooperative structural and electronic phenomena in solid state. They consist of populating nonequilibrium states by irradiating a system initially in its ground state. Once the photoexcitation is over, the material tends to relax from this photogenerated state. Several treatments that are proposed to interpret relaxation processes take advantage of the kinetic Ising-like model based on a stochastic approach developed by Boukheddaden and co-workers.[3–8] In particular, such a model turns out to be appropriate to allow for relaxations following light-induced excited spin state trapping (LIESST) effect in iron(II) spin-crossover complexes from a low-spin (LS) state ($^1A_1$) to a metastable high-spin (HS) state ($^5T_2$).[9,10] It accounts especially well for sigmoidal (self-accelerated) relaxation decays occurring in rather strongly cooperative systems. This kinetic Ising-like model has also the advantage to give a microscopic view of cooperative interactions, which is not the case in the empirical rate-equation model proposed by Hauser *et al.*,[11] even though it can reproduce the typical relaxation dynamics of iron(II) spin-crossover complexes (monoexponential and stretched exponential relaxations notably).

In this paper, we are going to focus on spin-crossover compounds showing double-step thermal spin transition. The two-sublattice Ising-like model suggested by Bousseksou *et al.*[12,13] is one of the best models used to explain the static behavior of their thermal spin conversion. In the frame of this approach, the double-step conversion is caused by the synergistic effect of ferromagneticlike and antiferromagneticlike interactions thought to be at the origin of the unusual photo-induced properties that are sometimes observed in these materials. Two interesting examples are the binuclear spin-crossover complex $[Fe(bt)(NCS)_2]_2(bpym)$ and the polymeric mononuclear spin-crossover complex $\{Fe(pmd)[Ag(CN)_2]Ag_2(CN)_3\}$. In the former, a double-step spin conversion from the HS-HS state to the LS-LS state via the HS-LS state occurs, and it is possible to populate selectively the HS-LS state using an infrared laser irradiation and the HS-HS state with a red laser excitation from the LS-LS state.[14–17] In the latter, the double-step relaxation behavior is also observed but only the pure HS state can be photogenerated.[18] In order to shed different light on the relaxations of double-step spin-crossover compounds, we extend in this paper the aforementioned kinetic Ising-like model to the study of relaxation processes from photo-induced states in double-step spin-crossover complexes by including local intra-site couplings.

In Sec. II, a different theoretical model based on microscopic Ising-like Hamiltonian including local antiferromag-

neticlike coupling is proposed using a stochastic master equation yielding a coupled system of differential dynamical equations. Computed results will be then presented in Sec. III, whereas Sec. IV is devoted to the explanation of relaxation curves of double-step spin-crossover system $[Fe(bt)(NCS)_2]_2(bpym)$ and $\{Fe(pmd)[Ag(CN)_2]Ag_2(CN)_3\}$. Section V concludes with the crucial points emphasized in this paper.

II. KINETIC TWO-SUBLATTICE ISING-LIKE MODEL

In this section, we introduce different dynamical equations to discuss relaxation processes. Our treatment is based on the stochastic method introduced by Glauber.[19] Despite the fact that detailed balance conditions provide several choices for transition probabilities, the relaxation rate is fully determined by a master equation, whatever this choice. Our method includes microscopic considerations as well, which allows a detailed time study of interaction effects inside the system.

A. Ising-like Hamiltonian of two-sublattice Ising-like model

The two-sublattice Ising-like model introduced by Bousseksou *et al.*[12] and consisted of the extended WP model[20] is an effective manner to reproduce double-step thermal spin conversion in spin-crossover complexes. The following model is based on a similar Ising-like Hamiltonian but is applied in the case of a system having local fictitious spin couplings,[13] such as binuclear or polymeric spin-crossover complexes. Considering two sublattices A and B, this Hamiltonian is given by Eq. (1),

$$H = J_1 \sum_{\langle i \neq j \rangle} \sigma_{iA}\sigma_{jA} + J_1 \sum_{\langle i \neq j \rangle} \sigma_{jB}\sigma_{iB} + J_2 \sum_{\langle i \neq j \rangle} \sigma_{iA}\sigma_{jB} + J_2 \sum_{\langle i \neq j \rangle} \sigma_{jA}\sigma_{iB} + J_{\text{local}} \sum_i \sigma_{iA}\sigma_{iB} + \sum_i \frac{\delta_A}{2}\sigma_{iA} + \sum_i \frac{\delta_B}{2}\sigma_{iB}. \tag{1}$$

The fictitious spin σ has the eigenvalues $\sigma = +1$ in the HS state, $\sigma = -1$ in the LS state, and the degeneracies u and r, respectively. Subscripts i and j stand for the site number and $\langle i \neq j \rangle$ means that all the different sites are taken into account only once in this sum. Each site i within sublattices A or B corresponds to the ith molecule of the binuclear compound [Fig. 1(a)]. In the case of polymeric spin-crossover systems, a set of neighboring dimerized atoms connected by covalent bonding is considered as i site [Fig. 1(b)]. Each binuclear complex or dimerized pair can take three possible states: HS-HS, HS-LS (LS-HS), and LS-LS states. We provide schemes of these molecular networks and corresponding Ising-like lattices in Fig. 1.

δ is associated to the ligand field energy difference between HS and LS states. J_1 and J_2 represent the magnitude of intersite interactions (intrasublattice and intersublattice, respectively). These interactions are thought to have long-range elastic origin in spin-crossover complexes. On the contrary, J_{local} expresses the magnitude of the short-range intrasite (intersublattice) interaction. This interaction should be related to the local molecular steric deformation or charge transfer between metal centers. It is worth noticing that the existence of this local coupling coming from covalent bonding is crucial in obtaining the double-step feature in the case of binuclear or polymeric complexes. In previous stochastic studies of two-sublattice Ising-like model,[6,8] only long-range interactions J_1 and J_2 were considered. J_1 was regarded as a ferromagneticlike interaction ($J_1 \geq 0$) and J_2 as an antiferromagneticlike interaction ($J_2 \leq 0$). These approaches were also able to reproduce double-step dynamics but could not treat the local coupling linked to covalent bonding. The rigorous treatment of the effect of intramolecular interactions J_{local} is the genuine asset of our model. We apply mean-field (MF) approximation only for intersite interactions (J_1, J_2). Intra-site interactions (J_{local}) are treated exactly to shed light on their role of paramount importance. This method is much more suitable for the binuclear system as discussed by Bousseksou *et al.*[13] The MF Hamiltonian is then rewritten as

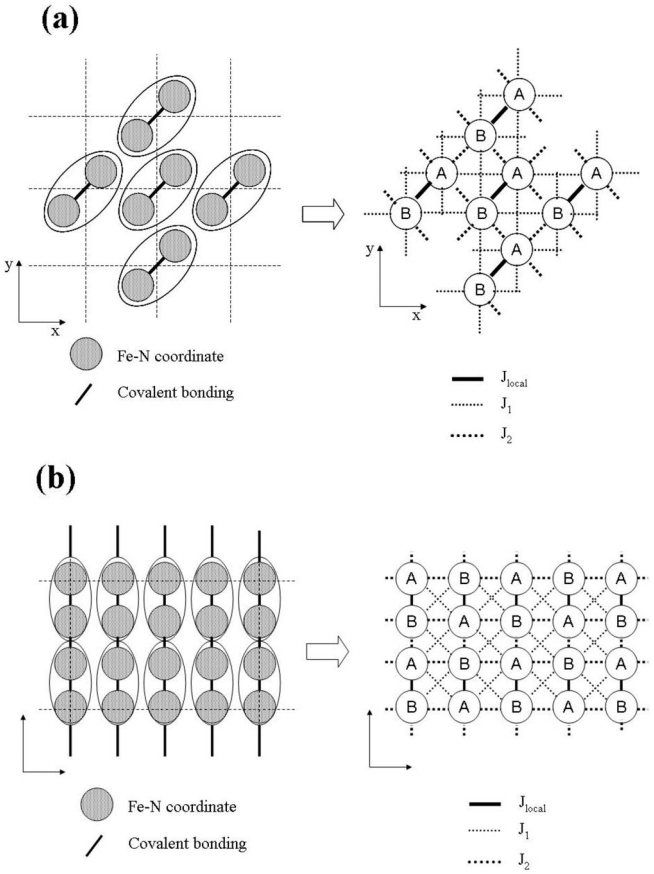

FIG. 1. Two-dimensional (2D) schemes of the molecular network in (a) $[Fe(bt)(NCS)_2]_2(bpym)$ and (b) $\{Fe(pmd)[Ag(CN)_2]Ag_2(CN)_3\}$ (left side). The corresponding two sublattices considered in our Ising-like model are shown in the right side.

$$H_{\text{MF}} \simeq \sum_i \left\{ -E_A\sigma_{iA} - E_B\sigma_{iB} + J_{\text{local}}\sigma_{iA}\sigma_{iB} - \frac{zJ_1}{2}(m_A^2 + m_B^2) - zJ_2 m_A m_B \right\}, \tag{2}$$

$$E_A = -(zJ_1 m_A + z' J_2 m_B + h_A), \tag{3}$$

$$E_B = -(z' J_2 m_A + zJ_1 m_B + h_B), \tag{4}$$

where $m_A = \langle \sigma_{iA} \rangle$ and $m_B = \langle \sigma_{iB} \rangle$ are the average values of each fictitious spin. z and z' are the numbers of nearest-neighbor sites. Here, we represent the zJ_1 ($z'J_2$) as J_1 (J_2) to simplify. The modified ligand field energy h_A is equal to $\frac{\delta_A}{2} - \frac{\ln(g_A)}{2\beta}$, $g_A = \frac{u_A}{r_A}$; h_B is equal to $\frac{\delta_B}{2} - \frac{\ln(g_B)}{2\beta}$, $g_B = \frac{u_B}{r_B}$, and $\beta = \frac{1}{k_B T}$. The term $\frac{\delta}{2}$ approximately corresponds to the enthalpy change ΔH at the thermal spin conversion. The term $\frac{\ln(g)}{2\beta}$ expresses the entropy change ΔS. u (r) expresses the degeneracy degree of HS (LS) state. Normally, spin degeneracy of HS state ($S=2$) should be 15 and that of LS ($S=0$) state should be 1. However, u and r are larger than these values because of the entropy change originated from molecular vibrations.

B. Master equation and stochastic treatment

The kinetic Ising-like model introduced by Glauber[19] is one of the best methods used to describe dynamical processes with Ising lattice. Boukheddaden and co-workers[3–6] first applied this stochastic treatment to spin-crossover systems and investigated additionally dynamical properties in double-step spin-crossover complexes.[6,8] However, their treatment did not include the term allowing for local couplings. In the following, we discuss the dynamical equations arising from the study of two-sublattice double-step spin-crossover complexes with local coupling based on Boukheddaden's method.

In this approach, each individual site interacts with a thermal bath whose state changes randomly. Here, the thermal bath spontaneously induces a fictitious spin flip from $\sigma_A(\sigma_B)$ to $-\sigma_A(-\sigma_B)$. The transition rate of the ith site is noted as $W(\sigma_{1A}, \cdots, \sigma_{iA}, \cdots, \sigma_{NA}:\sigma_{1B}, \cdots, \sigma_{NB} \rightarrow \sigma_{1A}, \cdots, -\sigma_{iA}, \cdots, \sigma_{NA}:\sigma_{1B}, \cdots, \sigma_{NB})$. Given the conversion from σ_{iA} to $-\sigma_{iA}$ and whatever the value of σ_{iB}, the dynamics is completely defined by the function W that is supposed to be independent of the historical account of the system (Markovian process). The time evolution of the probability $P(\sigma_{1A}, \cdots, \sigma_{iA}, \cdots, \sigma_{NA}:\sigma_{1B}, \cdots, \sigma_{NB})$ to be in the state $\{\sigma_{1A}, \cdots, \sigma_{iA}, \cdots, \sigma_{NA}:\sigma_{1B}, \cdots, \sigma_{NB}\}$ at time t is described by the master Eq. (5),

$$\begin{aligned}
\frac{d}{dt} P(\sigma_{1A}, \ldots \sigma_{iA}, \ldots, \sigma_{NA}:\sigma_{1B}, \ldots, \sigma_{iB}, \ldots, \sigma_{NB}; t) &= -\sum_i W(\sigma_{iA}, \sigma_{iB} \rightarrow -\sigma_{iA}, \sigma_{iB}) P(\sigma_{1A}, \ldots \sigma_{iA}, \ldots, \sigma_{NA}:\sigma_{1B}, \ldots, \sigma_{iB}, \ldots, \sigma_{NB}; t) \\
&\quad - \sum_i W(\sigma_{iA}, \sigma_{iB} \rightarrow \sigma_{iA}, -\sigma_{iB}) P(\sigma_{1A}, \ldots, \sigma_{iA}, \ldots, \sigma_{NA}:\sigma_{1B}, \ldots, \sigma_{iB}, \ldots, \sigma_{NB}; t) \\
&\quad + \sum_i W(-\sigma_{iA}, \sigma_{iB} \rightarrow \sigma_{iA}, \sigma_{iB}) P(\sigma_{1A}, \ldots, -\sigma_{iA}, \ldots, \sigma_{NA}:\sigma_{1B}, \ldots, \sigma_{iB}, \cdots, \sigma_{NB}; t) \\
&\quad + \sum_i W(\sigma_{iA}, -\sigma_{iB} \rightarrow \sigma_{iA}, \sigma_{iB}) P(\sigma_{1A}, \ldots, \sigma_{iA}, \ldots, \sigma_{NA}:\sigma_{1B}, \ldots, -\sigma_{iB}, \ldots, \sigma_{NB}; t).
\end{aligned} \tag{5}$$

At the equilibrium state, the derivative of $P(\sigma_{1A}, \cdots \sigma_{iA}, \cdots, \sigma_{NA}:\sigma_{1B}, \cdots, \sigma_{iB}, \cdots, \sigma_{NB}; t)$ becomes zero and yields the detailed balance conditions as follows:

$$\frac{W(\sigma_{iA}, \sigma_{iB} \rightarrow -\sigma_{iA}, \sigma_{iB})}{W(-\sigma_{iA}, \sigma_{iB} \rightarrow \sigma_{iA}, \sigma_{iB})} = \frac{P_e(-\sigma_{iA}, \sigma_{iB})}{P_e(\sigma_{iA}, \sigma_{iB})} = \frac{e^{-\beta E_A \sigma_{iA}} e^{\beta J_{\text{local}} \sigma_{iA} \sigma_{iB}}}{e^{\beta E_A \sigma_{iA}} e^{-\beta J_{\text{local}} \sigma_{iA} \sigma_{iB}}}, \tag{6}$$

$$\frac{W(\sigma_{iA}, \sigma_{iB} \rightarrow \sigma_{iA}, -\sigma_{iB})}{W(\sigma_{iA}, -\sigma_{iB} \rightarrow \sigma_{iA}, \sigma_{iB})} = \frac{P_e(\sigma_{iA}, -\sigma_{iB})}{P_e(\sigma_{iA}, \sigma_{iB})} = \frac{e^{-\beta E_B \sigma_{iB}} e^{\beta J_{\text{local}} \sigma_{iA} \sigma_{iB}}}{e^{\beta E_B \sigma_{iB}} e^{-\beta J_{\text{local}} \sigma_{iA} \sigma_{iB}}}. \tag{7}$$

Calculated from master Eq. (5), the time evolution of the averaged fictitious spin $m_A(m_B)$ and the correlation function become

$$\frac{d}{dt} m_A(t) = -2\langle \sigma_{iA} W(\sigma_{iA}, \sigma_{iB} \rightarrow -\sigma_{iA}, \sigma_{iB}) \rangle, \tag{8}$$

$$\frac{d}{dt} m_B(t) = -2\langle \sigma_{iB} W(\sigma_{iA}, \sigma_{iB} \rightarrow \sigma_{iA}, -\sigma_{iB}) \rangle, \tag{9}$$

$$\begin{aligned}
\frac{d}{dt} C(t) &= -2\langle \sigma_{iA} \sigma_{iB} W(\sigma_{iA}, \sigma_{iB} \rightarrow -\sigma_{iA}, \sigma_{iB}) \rangle \\
&\quad - 2\langle \sigma_{iA} \sigma_{iB} W(\sigma_{iA}, \sigma_{iB} \rightarrow \sigma_{iA}, -\sigma_{iB}) \rangle.
\end{aligned} \tag{10}$$

$C(t)$ corresponds to the intra-site correlation $\langle \sigma_{iA} \cdot \sigma_{iB} \rangle$. In order to solve these equations, the transition probability W

must be determined first. We emphasize that it is possible to choose any transition probability as long as it complies a detailed balance condition. However, in this paper, we only focus on Arrhenius-type dynamics because the relaxation of spin-crossover complexes is thought to be thermally activated.[3]

C. Dynamical choice

Among the distinct dynamical choices allowing the determination of the transition probability W, the "Arrhenius-type dynamics" leading to Eqs. (11) and (12) and the "Glauber dynamics" are well known. Boukheddaden *et al.*[3,4] already commented on the difference between Glauber and Arrhenius-type dynamics in the case of a mononuclear kinetic Ising-like model and they concluded that only Arrhenius-type dynamics could conveniently reproduce experimental data for highly cooperative spin-crossover materials and account for the thermally activated spin conversion process. In Arrhenius-type dynamics, the transition rate W should be

$$W(\sigma_{iA},\sigma_{iB} \rightarrow -\sigma_{iA},\sigma_{iB}) = k_A[\cosh(\beta E_A)\{1-\sigma_{iA}\tanh(\beta E_A)\}]e^{\beta J_{\text{local}}\sigma_{iA}\sigma_{iB}}, \tag{11}$$

$$W(\sigma_{iA},\sigma_{iB} \rightarrow \sigma_{iA},-\sigma_{iB}) = k_B[\cosh(\beta E_B)\{1-\sigma_{iB}\tanh(\beta E_B)\}]e^{\beta J_{\text{local}}\sigma_{iA}\sigma_{iB}}, \tag{12}$$

where k_A and k_B are the reaction rates related to the intramolecular energy barrier E^0_{act} and time constant τ_0.[3] The relation between k_A and these dynamical factors (E^0_{act} and τ_0) is expressed as follows: $k_A=\frac{e^{-\beta E^{0A}_{\text{act}}}}{2\tau^A_0}$ and $k_B=\frac{e^{-\beta E^{0B}_{\text{act}}}}{2\tau^B_0}$. The other parts of the transition probability behave as an additional activation energy derived from interactions and the energy difference between the HS and LS states.

D. Relaxation equations

After introducing Eqs. (11) and (12) into Eqs. (8)–(10), Eqs. (13)–(15) are deduced as follows:

$$\frac{d}{dt}m_A = k_A[\cosh(\beta J_{\text{local}})\{\sinh(\beta E_A)-m_A\cosh(\beta E_A)\} + \sinh(\beta J_{\text{local}})\{C(t)\sinh(\beta E_A)-m_B\cosh(\beta E_A)\}], \tag{13}$$

$$\frac{d}{dt}m_B = k_B[\cosh(\beta J_{\text{local}})\{\sinh(\beta E_B)-m_B\cosh(\beta E_B)\} + \sinh(\beta J_{\text{local}})\{C(t)\sinh(\beta E_B)-m_A\cosh(\beta E_B)\}], \tag{14}$$

$$\frac{d}{dt}C(t) = k_A[\cosh(\beta J_{\text{local}})\{m_A\sinh(\beta E_A)-\cosh(\beta E_A)\} + \sinh(\beta J_{\text{local}})\{m_B\sinh(\beta E_A)-C(t)\cosh(\beta E_A)\}] + k_B[\cosh(\beta J_{\text{local}})\{m_B\sinh(\beta E_B)-\cosh(\beta E_B)\} + \sinh(\beta J_{\text{local}})\{m_A\sinh(\beta E_B)-C(t)\cosh(\beta E_B)\}]. \tag{15}$$

These differential equations describe the relaxation process in the case of Arrhenius-type dynamics. The main point here lies in the possibility to evaluate the effect of local short-range interactions precisely. Equation (15) provides the time evolution of the fictitious spin correlation between two metal centers. We can solve Eqs. (13)–(15) numerically and derive three important parameters. The HS fraction $\gamma_{\text{HS}}(\equiv\frac{1}{2}+\frac{m_A+m_B}{4})$ is the first one. As discussed in previous papers,[8,13] $\Phi(t)(\equiv\frac{m_A(t)-m_B(t)}{2})$ is an order parameter reflecting antiferromagneticlike order (HS-LS order). This value is thought to express the degree of symmetry breaking. In the HS-LS state, molecules are ordered by either HS-LS or LS-HS. Once symmetry is breaking, the number of HS-LS species becomes larger (or smaller) than that of LS-HS species. $\Phi(t)$ expresses the degree of the bias of this molecular order. When $\Phi(t)$ is large, HS-LS species form a domain called "HS-LS ordered domain" thereafter. If $\Delta J(\equiv J_1-J_2)$ is larger than the threshold value ΔJ_{thres} (around 106 (K) in the binuclear system $[\text{Fe(bt)(NCS)}_2]_2\text{(bpym)}$), a symmetry breaking occurs and the order parameter Φ becomes finite.[12] Not only the value of J_{local} but also that of ΔJ conditions the occurrence of symmetry breaking thereby. The sign of $\Phi(t)$ refers to the direction of bias. If $\Phi(t)$ is negative, the LS-HS order domain is formed. On the other hand, $\gamma_{\text{HL}}(t)=\frac{1-C(t)}{2}$ allows for the density of the HS-LS pairs to be defined as follows:

$$\gamma_{\text{HL}}(t) = \frac{[\text{HS}-\text{LS}]+[\text{LS}-\text{HS}]}{[\text{HS}-\text{HS}]+[\text{HS}-\text{LS}]+[\text{LS}-\text{HS}]+[\text{LS}-\text{LS}]}. \tag{16}$$

Here, $[X]$ means the density of state X.

III. NUMERICAL CALCULATION

In this section, computed results from dynamical equations introduced in Sec. II are shown. First, we are going to investigate the effect of intermolecular and intramolecular interactions in the relaxation process of double-step complexes. Second, we are going to emphasize the role of symmetry breaking coming from the strong sensitivity to initial conditions of the dynamical equations or from the influence of asymmetry in sublattices.

A. Relaxation process from the photo-induced HS-HS state

Various relaxation curves from the photo-induced HS-HS state can be computed from Eqs. (13)–(15). Figure 2 depicts the schematic phase diagram in which each region corresponds to a particular number of inflection points in relax-

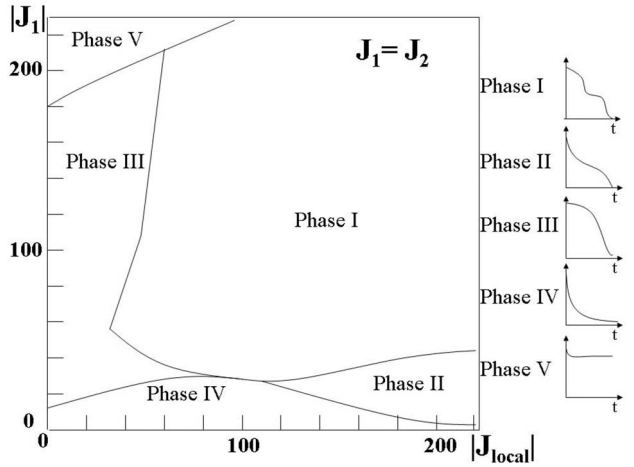

FIG. 2. Phase diagram of relaxation behavior when changing the magnitude of interactions at 50 K. The insets show the schematic relaxation curves for each phase. Parameters are set to $\delta_A=\delta_B=800$ (K), $g_A=g_B=200$, and $k_A=k_B=3.046\times10^{-6}$ (s^{-1}).

ation curves. It has been calculated in the assumption $J_1=J_2$ for the sake of simplicity. Sigmoidal double-step relaxation curves with three inflection points are obtained in Phase I. When J_{local} is strong but J_1 (or J_2) is weak, nonsigmoidal double-step relaxation curves with only two inflection points sometimes appear (Phase II). For weak J_{local} values, the plateau region disappears and a sigmoidal one-step conversion exhibiting only one inflection point is observed (Phase III). On the other hand, stretched exponential curves without inflection points are observed when both J_1 and J_{local} are weak (Phase IV). In Phase V, the LS-LS state is not the ground state at low temperature, and relaxation curves go flat at an intermediate HS fraction.

Figure 3(a) shows relaxation curves with increasing values of the long-range interactions J_1 ($J_1=J_2$), i.e., on going from Phase IV to Phase I. When decreasing the absolute value of J_1, the relaxation becomes more and more gradual, that is, mono-exponential-like. This results from the progressive disappearance of ferromagneticlike intersite interactions. In contrast, Fig. 3(b) reveals the dependence of relaxation curves versus the short-range interaction J_{local}. The duration of the first step of the relaxation decay, i.e., the lifetime of HS-HS pairs, shortens more and more with the increase in J_{local} and the duration of the second step, i.e., the lifetime of HS-LS pairs, lengthens. This stems from the fact that the antiferromagneticlike intra-site interaction J_{local} promotes the formation of the HS-LS pairs. Taking J_{local} into account turns out to be crucial in reproducing HS-LS plateaus while J_1 (and J_2) merely affects the time scale of the two relaxation steps. Similar conclusions could be inferred for distinct values of J_1 and J_2.

Figure 4 provides a typical double-step relaxation curve $[\gamma_{\text{HS}}(t)]$ accompanied by the time dependence of $\gamma_{\text{HL}}(t)$ and $\Phi(t)$ [case $(\Delta g \equiv g_A - g_B)=0$]. At $t=0$, the correlation term $C(0)$ should be around 1 because fluctuations are rather small. The HS-LS fraction $\gamma_{\text{HL}}(0)$ is almost zero. At the onset of the relaxation process, the photo-induced HS-HS state is very stable because of cooperative long-range elastic interactions. Nevertheless, once the relaxation starts, the spin

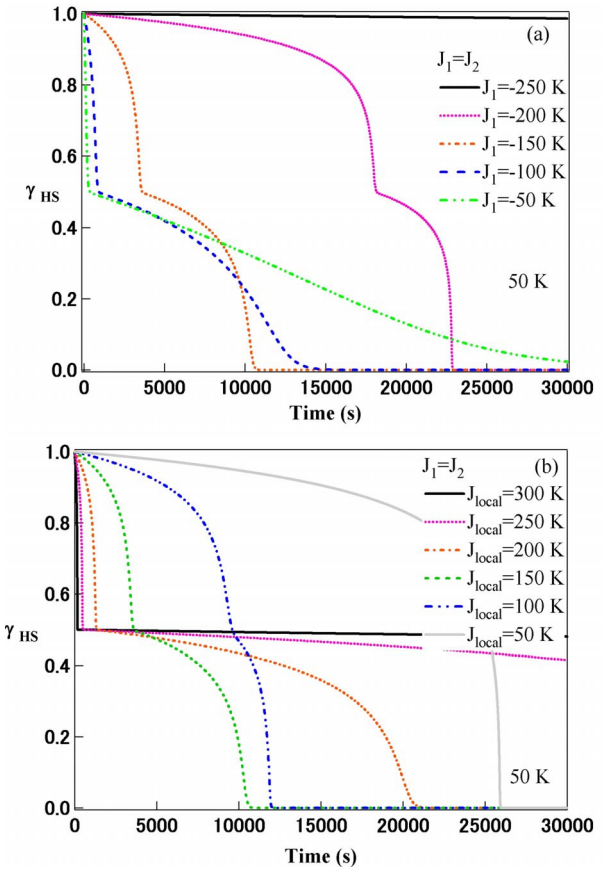

FIG. 3. (Color online) Relaxation curves from the HS-HS state at 50 (K) computed in the case where $J_1=J_2$ for several values of (a) J_1 [$J_{\text{local}}=150$ (K)] and (b) J_{local} [$J_1=-150$ (K)]. $\delta_A=\delta_B=800$ (K), $g_A=g_B=200$, and $k_A=k_B=3.046\times10^{-6}$ (s^{-1}).

conversion rapidly accelerates and reaches a plateau at about ($\gamma_{\text{HS}}=0.5$). At this plateau, almost all molecules are in the HS-LS state ($\gamma_{\text{HL}}\sim1$). Moreover, Φ is thoroughly zero, which means that the order of HS-LS pairs is completely random. It is however possible to obtain ordered HS-LS pairs as explained in Secs. III B and III C.

B. Asymmetric effect

In the previous part, we supposed that sublattices A and B were perfectly equivalent. However, in the investigated double-step complexes, molecules forming a dimer are not equivalent. Such a difference between sublattices A and B can be modeled by using asymmetrical parameters h_A and h_B with $h_A \neq h_B$. This involves the introduction of an asymmetry in the enthalpy or the entropy terms. Thereafter, we focus only on an entropy change but the same conclusions could be reached considering an enthalpy modification between sublattices A and B. Figure 4(a) shows the computed relaxation curves from the HS-HS state at 50 K when $g_A(=150)$ is not equal to g_B, that is to say taking into account a difference in entropy between the two sublattices. The corresponding time evolution of the HS-LS fraction γ_{HL} and the symmetry-breaking parameter Φ are drawn in Figs. 4(b) and 4(c), respectively. When the absolute value of Δg is small (Δg

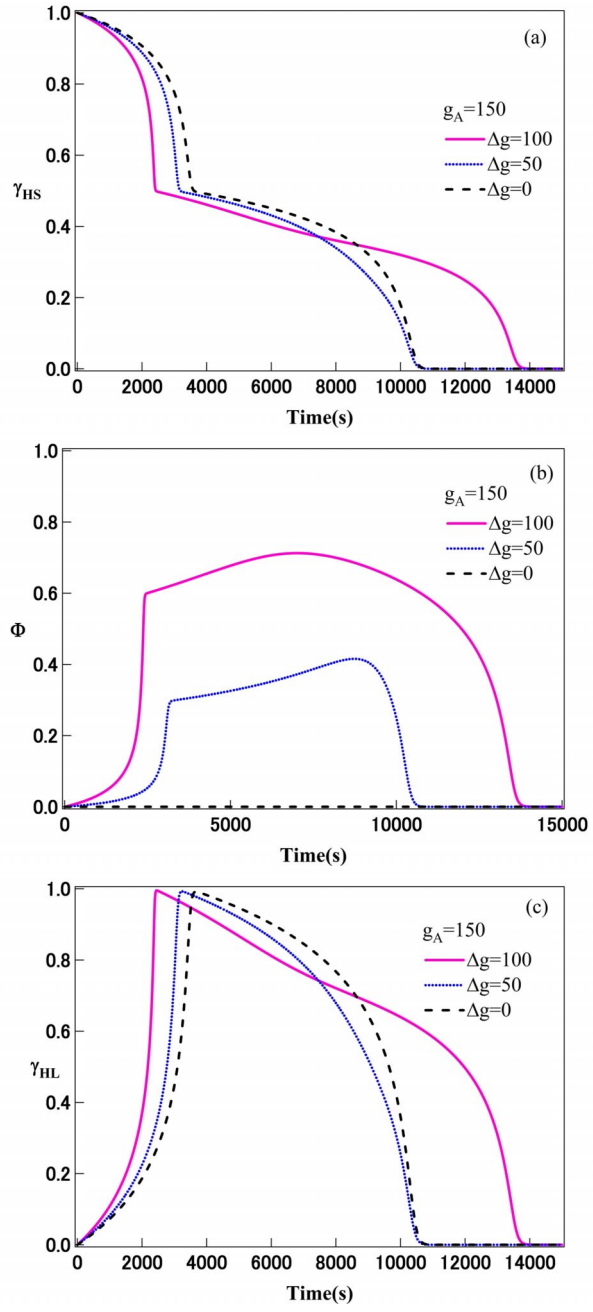

FIG. 4. (Color online) (a) Computed relaxation curves from the HS-HS state. Time dependence (b) of the symmetry-breaking parameter Φ and (c) of the HS-LS fraction at 50 (K) for $\Delta g=0$, 50, and 100. g_A is fixed at 150. $J_1=J_2=-150$ (K) and $J_{\text{local}}=150$ (K). Other parameters are fixed at the same values as in Fig. 3.

=50), the ordinary double-step relaxation tied to minor changes in Φ appears. γ_{HS} decreases to 0.5 while Φ increases to 0.3 first. In the meantime, γ_{HL} reaches 1. These results indicate that all the molecules become HS-LS even if the HS-LS ordered domain is not really extended. Since then, γ_{HS} relaxes to 0 concomitantly to the decrease in Φ and γ_{HL}. The system falls down in its LS-LS state. When the absolute value of Δg is large enough, nonetheless ($\Delta g=100$), a triple-step behavior appears. As shown in Fig. 4, γ_{HS} initiates its final decrease, i.e., its third step, as soon as Φ reaches its maximum. This triple-step process comes from the obtention of a parameter Φ up to twice as large as in the case of $\Delta g=50$. As $\Phi(t)$ corresponds to the degree of symmetry breaking, which relates to the total area of the HS-LS ordered domain, its time evolution expresses the generation and expansion of HS-LS ordered domain. In this case, an HS-LS (or LS-HS) ordered domain is formed at the plateau and lengthens the lifetime of HS-LS pairs thereby.

C. Symmetry breaking caused by initial fluctuations

Albeit a symmetry breaking is rendered possible for an asymmetric system, it can occur for a symmetric one as well. In this event, the symmetry breaking originates from fluctuations in the initial state. If sites *A* and *B* are perfectly equivalent, $\Phi(t)$ should be zero when the initial condition $\Phi(0)=0$. Nevertheless, in case of small fluctuations in the initial photo-induced state, the symmetry breaking at time zero is progressively enhanced. When $\Phi(0)$ is not zero [$\Phi(0)=0.0005$], the relaxation curves of $\gamma_{HS}(t)$ exhibit a triple instead of a double-step behavior (Fig. 5). $\gamma_{HL}(t)$ and $\Phi(t)$ increase gradually at first while $\gamma_{HS}(t)$ decreases. As soon as it reaches almost 1, $\gamma_{HL}(t)$ starts decreasing and the increase rate of $\Phi(t)$ changes. Subsequently, $\Phi(t)$ approaches $\gamma_{HL}(t)$. When $\Phi(t)$ is equal to $\gamma_{HL}(t)$, the decay rate of $\gamma_{HS}(t)$ slightly diminishes. At the first stage, the HS-LS state (in fact HS-LS or LS-HS species) is produced randomly during the relaxation process. Then, HS-LS ordered domains are formed and grow little by little. Finally, all the HS-LS molecules order themselves in the same direction. We should add, however, that $\Phi(t)$ expresses the total area of HS-LS ordered domains and the size of each single domain cannot be estimated. Furthermore, the triple-step behavior only occurs for large enough values of $\Delta J \equiv J_1 - J_2$ and J_{local}.

When $\Phi(0)$ becomes larger than 0.0025, an atypical relaxation proceeds (Fig. 5). HS-LS pairs are formed immediately since γ_{HS} decreases to 0.5 but, instead of relaxing to the LS-LS state, HS-LS ordered domains are rapidly generated and lead to an HS-LS ordered state. To explain this curious dynamics, the contour plot of the free energy is shown in Fig. 6 together with the projection of the three-dimensional (3D) (m_A, m_B, C) path in the $(m_A m_B)$ plane. The free energy at $(m_A, m_B)=(1,-1)$ (HS-LS state) is slightly higher than that at $(m_A, m_B)=(-1,-1)$ (LS-LS state) but much lower than the free energy at $(m_A, m_B)=(1,1)$ (HS-HS state). The LS-LS state is consequently the ground state of this material as expected. However, the point $(m_A, m_B)=(1,-1)$ is also stable because the temperature is too low to pass over the energy barrier between $(m_A, m_B)=(-1,-1)$ and $(m_A, m_B)=(1,-1)$. If the 3D path can cross the bifurcation line (red dashed line), the final destination becomes the LS-LS ground state $(m_A, m_B)=(-1,-1)$ [red line computed for $m_B(0)=0.999$]. Otherwise, the system goes to the metastable HS-LS state $(m_A, m_B)=(1,-1)$ [blue line computed for $m_B(0)=0.995$]. The destination of the relaxation path is consequently different when the initial configuration is slightly modified. This also implies that a selective photoswitching could be realized, in principle, using double-step spin-crossover materials.

IV. COMPARISON WITH EXPERIMENTAL RESULTS

In this section we propose a comparison between experimental and simulated relaxation curves in the bi-

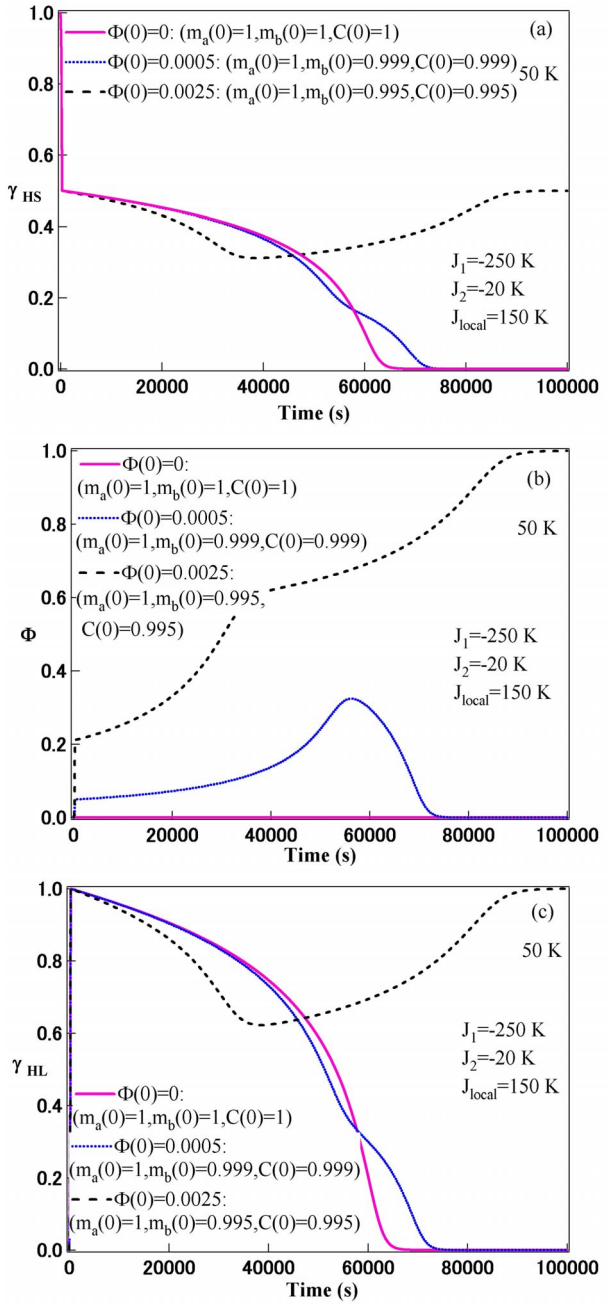

FIG. 5. (Color online) (a) Computed relaxation curves from the HS-HS state. Time dependence (b) of the symmetry-breaking parameter Φ and (c) of the HS-LS fraction at 50 K for a symmetry-breaking parameter Φ(0) equal to 0, 0.0005, and 0.0025, initially. Interaction parameters are set to $J_1=-250$ (K), $J_2=-20$ (K), and $J_{\text{local}}=150$ (K). Other parameters remain the same as in Fig. 3.

nuclear $[Fe(bt)(NCS)_2]_2$ and the polymeric $\{Fe(pmd)[Ag(CN)_2]Ag_2(CN)_3\}$ spin-crossover complexes. As a first step, thermal spin transitions of $[Fe(bt)(NCS)_2]_2(bpym)$ and $\{Fe(pmd)[Ag(CN)_2]Ag_2(CN)_3\}$ are discussed to estimate the relevant parameters for the following dynamical treatment. δ and g are, respectively, determined from the enthalpy and the entropy associated to each step of the spin transition.[18,21] On the contrary, the interaction parameters J_1, J_2, and J_{local} are obtained by making the

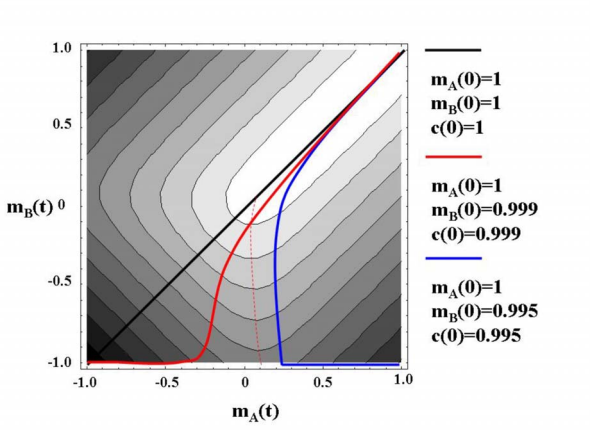

FIG. 6. (Color online) Contour plot of the free energy and projections of the 3D ($m_A m_B C$) path in the ($m_A m_B$) plane for distinct initial parameters: $m_A(0)=m_B(0)=C(0)=1$ (black); $m_A(0)=1$, $m_B(0)=C(0)=0.999$ (red); $m_A(0)=1$, $m_B(0)=C(0)=0.995$ (blue).

shape of the thermal spin crossover match the experimental transition. However, such a set of parameters is shown to be inadequate to reproduce experimental relaxations. To manage a good agreement, interaction parameters must be reduced by a constant factor, which is dependent on the material and whose origin will be also discussed.

A. Binuclear spin-crossover complex $[Fe(bt)(NCS)_2]_2(bpym)$

In the binuclear spin-crossover complex $[Fe(bt)(NCS)_2]_2(bpym)$ shown in the left side of Fig. 1(a), a molecule is composed of two Fe-N coordinates linked by a covalent bond. Each molecule looks isolated but connects each other through intermolecular interactions. It shows a double-step thermal spin conversion from the HS-HS to the LS-LS state via the HS-LS state.[21] Steps 1 and 2 are centered around 163 and 197 (K), respectively. The former is abrupt and the latter is gradual. This material should be adequate to apply our model accordingly. Real *et al.*[21] showed that the enthalpy change was different in each step, $\Delta H_A=7.9$ (kJ/mol) and $\Delta H_B=5.4$ (kJ/mol). Generally, the change of enthalpy ΔH determined by the heat-capacity measurement should include not only the values of δ_A and δ_B but also J_1, J_2, and J_{local}. However, the amount of interaction parameters (J_1, J_2, and J_{local}) is much smaller than the energy gap because the sign of J_1 and J_2 is opposite to that of J_{local}. It is natural that the contribution of interactions to the enthalpy change ΔH is negligible. Therefore, we suppose that ΔH_A is equal to $\frac{\delta_A}{2}$ and ΔH_B is equal to $\frac{\delta_B}{2}$. This leads to $\delta_A=1014$ (K) and $\delta_B=710$ (K). On the other hand, the entropy change ΔS_A (ΔS_B) is attributed to the term of logarithm of degenerate factor g_A (g_B) as already pointed out by Bousseksou *et al.*[12,13] The entropy change of each step was around 42 (J/mol K). This leads to $g_A=130$ and $g_B=130$.

Parameters J_1, J_2, and J_{local} are deduced by trying to reproduce as reliably as possible the thermal transition using a two-sublattice model. In our case, $J_1=-130$ (K), $J_2=-130$ (K), and $J_{\text{local}}=85$ (K) turn out to be suitable param-

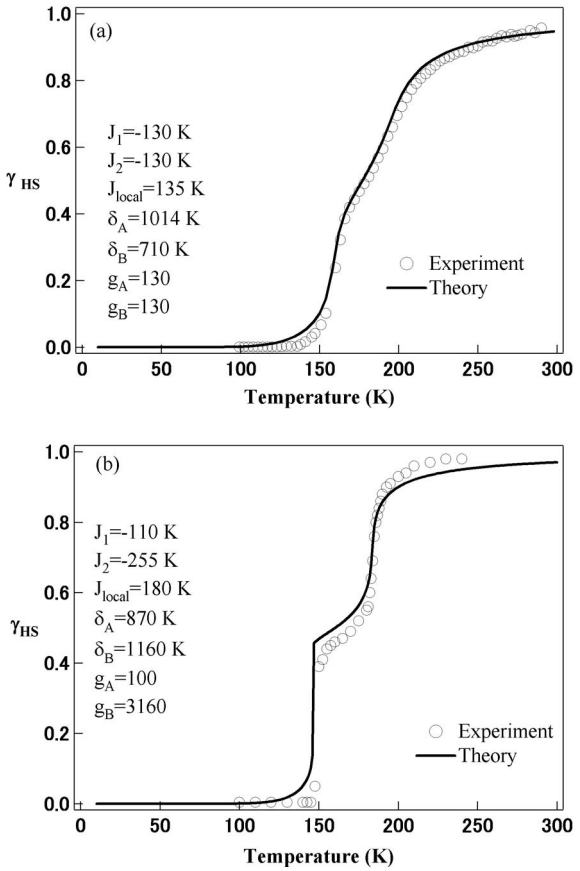

FIG. 7. Spin transition curves of (a) the binuclear spin-crossover complex $[Fe(bt)(NCS)_2]_2(bpym)$ and (b) the polymeric spin-crossover complex $\{Fe(pmd)[Ag(CN)_2]Ag_2(CN)_3\}$. Open circles are derived from magnetic measurement in (a) and optical measurement in (b). Red lines are computed from our model. Relevant parameters are written in the figures.

eters. It is noteworthy that different parameters were used in a previous study about $[Fe(bt)(NCS)_2]_2(bpym)$ (Ref. 12) but in this case the difference in enthalpy for each step was not considered. Figure 7(a) provides the thermal spin conversion curves of $[Fe(bt)(NCS)_2]_2(bpym)$. Open circles stand for the experimental data and red solid lines for the simulated curves.

Letard and co-workers[14,15] discovered first the LIESST phenomenon from the LS-LS state to the HS-HS state in this material. They indicated that visible light (647 nm) brought LS-LS molecules to the HS-HS state below 70 (K). Later, we have demonstrated that a near infrared source (1342 nm) enabled to reach HS-LS molecules from the LS-LS state.[16] This interesting selective photoswitching effect has been confirmed by several experiments, such as magnetic-susceptibility measurements, Raman scattering, infrared absorption, and x-ray diffraction.[16,17] All experimental data strongly suggested that the infrared excitation state was HS-LS but did not imply any symmetry breaking. We acquired infrared-absorption spectra to look into the dynamics of photo-induced states in the above-mentioned binuclear spin-crossover complex. The forthcoming determination of the high-spin fraction γ_{HS} was conveniently performed using CN stretching modes which are sensitive to changes of the spin state. These spectra were acquired by means of a Shimadzu Prestige-21 Fourier transform infrared (FTIR) spectrometer. The powder sample was embedded in a KBr pellet. The calibrating light of the He-Ne laser was obstructed by a needle. We populated the HS-HS state using a visible laser light source (CW: YAG laser, 532 nm or laser photodiode, 785 nm) and the HS-LS state using an infrared laser light source (CW: YVO_4 laser: 1342 nm). In order to investigate the relaxation process, we generated photo-induced HS-HS and photo-induced HS-LS states using red or infrared irradiation at 10 (K) and heated the sample to measurement temperature under irradiation. The closed triangles in Fig. 8(a) displays the time evolution of the HS fraction of this compound recorded at several temperature. These curves look like stretched exponentials. They are very similar to the relaxation curves obtained by Chastanet *et al.*[15] by means of magnetic-susceptibility measurements. Solid lines in Fig. 8(a) show the computed relaxation curves from the photo-induced HS-HS state using parameters directly determined by fitting the thermal spin transition. All computed curves are double-step sigmoidals far from the desired stretched exponentials experimentally observed. Reaction rates k_A and k_B are temperature dependent but it is possible to extract the values of E_{act}^{0A}, τ_0^A, E_{act}^{0B}, and τ_0^B by means of a simple Arrhenius plot providing $\ln(k) = -E_{act}^{0i}/T - \ln 2\tau_0^i$ $(i=A$ or$B)$ as a function of $1/T$.[22] Here, we set these parameters as $E_{act}^{0A} = 1158$ (K), $\tau_0^A = 1.0 \times 10^{-4}$, $E_{act}^{0B} = 1089$ (K), and $\tau_0^A = 6.7 \times 10^{-4}$, which give rise to best fitting curves. However, the deviation from experimental results is conspicuous. Moreover, E_{act}^{0A} should be equal to E_{act}^{0B}. Generally speaking, the two sublattices A and B are equivalent in the binuclear spin-crossover system because of molecular symmetry.

As already discussed in Sec. III, a stretched exponential relaxation curve is obtained when both J_1 and J_{local} are weak. Then we should reduce interaction parameters to fit the experimental curves. Parameters δ_A, δ_B, g_A, and g_B must remain identical. However, all parameters should be weakened evenly because every dimerized pair is equivalent at the microscopic scale. We are looking for suitable relaxation curves by varying the reaction rates k_A (or k_B) and the reducing parameter a, hence. The meaning of reduced parameter a is discussed in Sec. IV B. These reaction rates are slightly different depending on whether the relaxation starts from the HS-HS state or the HS-LS state. We can estimate that the intramolecular energy barrier is $E_{act}^{0A} = E_{act}^{0B} = 1205$ (K) and the time constant is $\tau_0^A = \tau_0^B = 3.3 \times 10^{-4}$ (s) for the relaxation from the HS-HS state. These values can be assessed to $E_{act}^{0A} = E_{act}^{0B} = 1164$ (K) and $\tau_0^A = \tau_0^B = 2.2 \times 10^{-4}$ (s) for the relaxation from the HS-LS state. The difference between the relaxation from HS-LS and that from HS-HS might be attributed to the quality of the KBr pellet. The optimized factor a is equal to 4. Considering the aforementioned k_A and k_B, the reduced interaction parameters, $\frac{J_1}{a} = -32.5$ (K), $\frac{J_2}{a} = -32.5$ (K), and $\frac{J_{local}}{a} = 21.25$ (K), allow the relaxation curves from HS-HS and the HS-LS states to reproduce nicely as shown in Figs. 8(b) and 8(c), respectively.

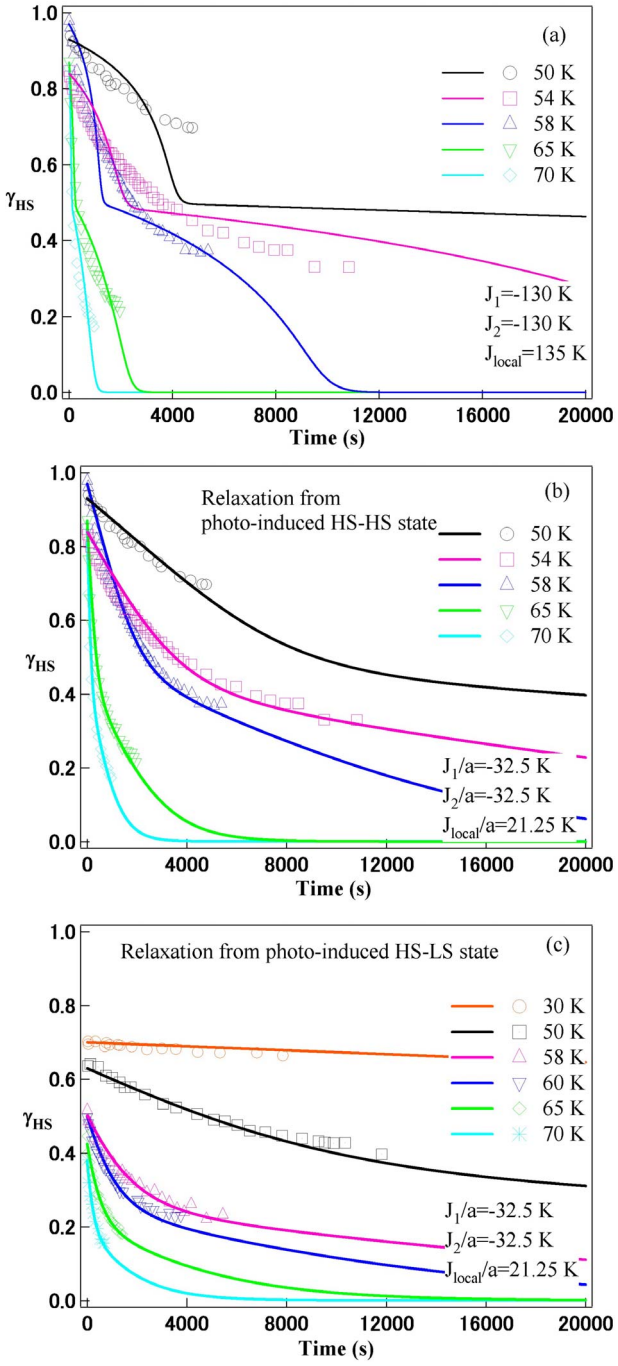

FIG. 8. (Color online) (a) Experimental relaxation curves from photo-induced HS-HS state of $[Fe(bt)(NCS)_2]_2(bpym)$ at several temperatures obtained from infrared-absorption experiments (triangles) and simulated relaxation curves at the same temperature. Parameters are the same as in Fig. 7(a). (b) Experimental relaxation curves from the photo-induced HS-HS state of $[Fe(bt)(NCS)_2]_2(bpym)$ at several temperatures obtained from infrared-absorption experiment (triangles) and simulated relaxation curves at the same temperature using reduced interaction parameters. (c) Experimental relaxation curves from the photo-induced HS-LS state of $[Fe(bt)(NCS)_2]_2(bpym)$ at several temperatures obtained from infrared-absorption experiment (triangles) and simulated relaxation curves at the same temperature using reduced interaction parameters.

B. Polymeric spin-crossover complex $\{Fe(pmd)[Ag(CN)_2]Ag_2(CN)_3\}$

By means of crystallographic measurements, Niel *et al.*[18] demonstrated that each unit cell of $\{Fe(pmd)[Ag(CN)_2]Ag_2(CN)_3\}$ contains five crystallographically inequivalent iron atoms called Fe(1), Fe(2), Fe(3), Fe(4), and Fe(5). Moreover, this material exhibits an abrupt double-step thermal spin transition whose critical temperatures are 185 and 148 K for the high-temperature and the low-temperature steps, respectively. The thermal spin transition of Fe(5) from the HS to the LS state starts at a slightly higher temperature than for the other iron centers. However, the five iron centers can thermodynamically be sorted into two sets. The first contains Fe(3), Fe(5), and half of the Fe(1) atoms, which undergo the spin-crossover transition during the high-temperature step. The second set contains Fe(2), Fe(4), and the other half of Fe(1), which undergo the spin-crossover transition during the low-temperature step. In this context, it turns out that it is possible to ascribe each set of iron atoms to a particular sublattice and to apply our model [see left side of Fig. 1(b)]. Each sublattice (A and B) is characterized by a distinct value of the energy difference δ, the degeneracy g, the time constant τ_0, and the activation energy barrier E^0_{act}. In principle, the interaction parameters J_1 and J_2 can be different as well depending on whether we consider the effect of A sites on B sites or the opposite. δ and g are, respectively, determined from the enthalpy and the entropy associated to each step of the spin transition.[18] The enthalpy changes $\Delta H_1=7.2$ (kJ/mol) and $\Delta H_2=9.6$ (kJ/mol) and the entropy changes $\Delta S_1=38.0$ (J/mol K) and $\Delta S_2=67.0$ (J/mol K) lead to $\delta_A=870$ (K), $\delta_B=1160$ (K), $g_A=100$, and $g_B=3160$. Parameters $J_1=-110$ (K), $J_2=-250$ (K), and $J_{local}=180$ (K) are deduced by tempting to reproduce as reliably as possible the thermal transition using a two-sublattice model. The high value of J_{local} is especially crucial to obtain a steep thermal transition at the low-temperature step [Fig. 7(b)].

Closed triangles of Fig. 9(a) indicate the relaxation curves from the photo-induced state determined from optical measurements performed by Real and co-workers.[18] A neat double-step relaxation takes place in this material on the whole investigated temperature range. The relaxation curves calculated by means of the set of parameters optimized through the fitting procedure of the thermal spin crossover [Fig. 7(b)] are also reported in Fig. 9(a). In comparison with $[Fe(bt)(NCS)_2]_2(bpym)$, the agreement between experiments and theory seems to be better. $E^{0A}_{act}=945$ K and $E^{0B}_{act}=972$ (K) and the time constants $\tau^A_0=2.7\times10^{-3}$ (s) and $\tau^B_0=1.3\times10^{-5}$ (s) are obtained using an Arrhenius plot. However, the small difference between calculation and experimental curves is still existing. To remove this gap, a reduction factor of interaction parameters $b=1.38$ might be introduced as well. As displayed in Fig. 9(b), the parameters $J_1/b=-80$ (K), $J_2/b=-185$ (K), and $J_{local}/b=135$ (K) can reproduce conveniently the experimental relaxation curves if considering this factor. For these simulations, the reaction rates k_A and k_B yield the activation energy barriers $E^{0A}_{act}=1162$ (K) and $E^{0B}_{act}=999$ (K) and the time constants $\tau^A_0=1.8\times10^{-4}$ (s) and $\tau^B_0=8.0\times10^{-4}$ (s) using an Arrhenius plot as in Sec. IV A.

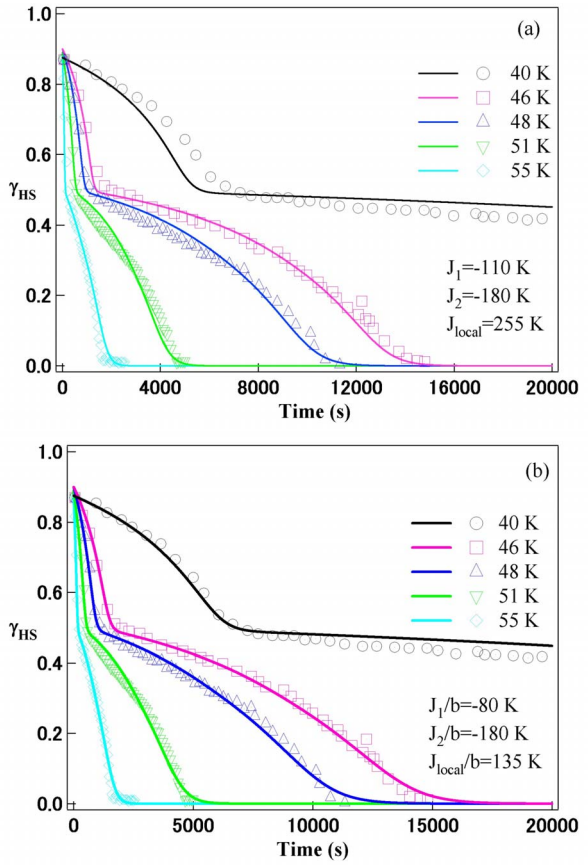

FIG. 9. (Color online) (a) Experimental relaxation curves from the photo-induced state of $\{Fe(pmd)[Ag(CN)_2]Ag_2(CN)_3\}$ at several temperatures obtained from optical measurements (triangles) and simulated relaxation curves at the same temperature. Experimental results have been extracted from the literature (Ref. 18) Parameters are the same as in Fig. 7(b). (b) Experimental relaxation curves from the photo-induced state of $\{Fe(pmd)[Ag(CN)_2]Ag_2(CN)_3\}$ at several temperatures obtained from optical measurements (triangles) and simulated relaxation curves at the same temperature using reduced interaction parameters $J_1/b=-80$ (K), $J_2/b=-185$ (K), and $J_{local}/b=135$ (K).

Obviously, the reduced parameter is effective as the case of binuclear spin-crossover complex $[Fe(bt)(NCS)_2]_2(bpym)$. However, in the case of polynuclear complex, we could reproduce the relaxation behavior without supposing reduced parameter to some extent. Therefore, we do not know if the reduced factor is always needed but the fact is that the introduction of reduced parameter yields slightly better fitting curves. This means that the supposition of reduced parameter cannot make the situation too bad. Then, we believe that the introduction of reduced factor is the universal method. We discuss the origin of this factor in Sec. IV C.

C. Discussion

As mentioned in Sec. IV B, the use of mean-field kinetic Ising-like model to explain the relaxation process of double-step spin-crossover systems requires the introduction of reduced interaction parameters. Such a reduction may originate from several phenomena. (1) The investigated temperature ranges are not fully in the thermally activated region. In this assumption, the relaxation would be affected by the temperature-independent tunneling effect especially at the lowest temperatures between 30 and 50 K. As this effect does not play any role in the thermal transition, it could only influence the values of interaction parameters used to fit relaxation curves.[18] (2) A large inhomogeneous distribution of zero-point energy difference may exist. This is particularly true for spin-crossover materials exhibiting stretched exponential relaxations[23] but has also been suggested for the spin-crossover complex $\{Fe(pmd)[Ag(CN)_2]Ag_2(CN)_3\}$.[18] (3) Light-induced inhomogeneities may appear. The double-step spin-crossover materials are quite well ordered at thermal equilibrium. Nevertheless, the network expansion generated by laser photoexcitation from the LS-LS to the HS-HS state could produce crystal distortions and give rise to inhomogeneities. These inhomogeneities could alter the relaxation process and involve consequently the consideration of a smaller fictitious spin coupling to improve the accordance between measurements and calculations. (4) The mean-field approximation may be less relevant at the photo-induced state. In a steady state, at the equilibrium, the mean-field approximation really makes sense because the spin transition occurs faster than the perturbation of the system. On the contrary, significant fluctuations occur for a photo-induced state because it is far from equilibrium. In such a situation, neighboring spins only provide information on a very localized region and interaction parameters are reduced thereby.

V. CONCLUSION

We have proposed a different theoretical approach based on a stochastic method to account for relaxation processes in double-step spin-crossover complexes. The main difference of the theoretical treatment lies in the introduction of short-range intra-site correlations between metal centers. For a strong correlation, the antiferromagneticlike intra-site interaction J_{local} dominates the system and stabilizes the HS-LS state. In addition, ferromagneticlike intermolecular interactions J_1 and J_2 can deeply affect the shape of the relaxation as well. The time evolution of the symmetry-breaking parameter Φ and the fraction of the HS-LS pairs γ_{HL} have been calculated simultaneously. The symmetry breaking coming from the asymmetry between sublattices A and B or fluctuations in the initial photoexcited state yields atypical relaxation behaviors. In both cases, triple-step relaxation processes have been obtained but weak initial fluctuations can also lead to a final HS-LS state instead of the LS-LS ground state. The latter results indicate that the control of initial fluctuations should allow one to populate hidden photo-induced states, such as the aforementioned metastable HS-LS state.

Experimental relaxation curves of $[Fe(bt)(NCS)_2]_2(bpym)$ and $\{Fe(pmd)[Ag(CN)_2]Ag_2(CN)_3\}$ could not be reproduced directly with the interaction parameters determined from the fitting procedure of their thermal transition. However, a reduction of interaction parameters renders a possible excellent

agreement between theory and experiment in the frame of our model. Both the stretched exponential decays observed in $[Fe(bt)(NCS)_2]_2(bpym)$ and the marked double-step relaxations in $\{Fe(pmd)[Ag(CN)_2]Ag_2(CN)_3\}$ can be reproduced, which is quite remarkable. This mandatory reduction may be ascribed to the occurrence of temperature-independent tunneling effect to some extent at the lowest temperatures, to the presence of a large inhomogeneous distribution of zero-point energy difference or light-induced inhomogeneities, and also to the considered mean-field approximation itself.

ACKNOWLEDGMENTS

One of the authors (S.M.) has been supported by the CDFJ (Collège doctoral franco-japonais) program for studying in LCC/CNRS in Toulouse. The authors are also grateful to the JSPS for a grant provided to N.O.M. This work was supported by Grant-in-Aid for Creative Scientific Research and the 21st Century COE Program "Center for Diversity and Universality in Physics" from MEXT. The authors are indebted to J. A. Real for the experimental data about $\{Fe(pmd)[Ag(CN)_2]Ag_2(CN)_3\}$.

*Corresponding author; 3c273@scphys.kyoto-u.ac.jp
†kochan@scphys.kyoto-u.ac.jp
‡boussek@lcc-toulouse.fr

[1] *Photo-Induced Phase Transition*, edited by K. Nasu (World Scientific, Singapore, 2004).
[2] S. Koshihara, Y. Tokura, T. Mitani, G. Saito, and T. Koda, Phys. Rev. B **42**, 6853 (1990).
[3] K. Boukheddaden, I. Shteto, B. Hôo, and F. Varret, Phys. Rev. B **62**, 14796 (2000).
[4] B. Hôo, K. Boukheddaden, and F. Varret, Eur. Phys. J. B **17**, 449 (2000).
[5] K. Boukheddaden, J. Linares, H. Spiering, and F. Varret, Eur. Phys. J. B **15**, 317 (2000).
[6] K. Boukheddaden, J. Linares, E. Codjovi, F. Varret, V. Niel, and J. A. Real, J. Appl. Phys. **93**, 7103 (2003).
[7] S. Miyashita, Y. Konishi, M. Nishino, H. Tokoro, and P. A. Rikvold, Phys. Rev. B **77**, 014105 (2008).
[8] M. Nishino, K. Boukheddaden, S. Miyashita, and F. Varret, Phys. Rev. B **68**, 224402 (2003).
[9] *Topics in Current Chemistry*, edited by P. Gütlich (Springer-Verlag, Berlin, 2004).
[10] Y. Ogawa, S. Koshihara, K. Koshino, T. Ogawa, C. Urano, and H. Takagi, Phys. Rev. Lett. **84**, 3181 (2000).
[11] A. Hauser, P. Gütlich, and H. Spiering, Inorg. Chem. **25**, 4245 (1986).
[12] A. Bousseksou, J. Nasser, J. Linares, K. Boukheddaden, and F. Varret, J. Phys. I **2**, 1381 (1992).
[13] A. Bousseksou, F. Varret, and J. Nasser, J. Phys. I **3**, 1463 (1993).
[14] J.-F. Letard, J. A. Real, N. Moliner, A. B. Gaspar, L. Capes, O. Cador, and O. Kahn, J. Am. Chem. Soc. **121**, 10630 (1999).
[15] G. Chastanet, C. Carbonera, C. Mingotaud, and J.-F. Letard, J. Mater. Chem. **14**, 3516 (2004).
[16] N. O. Moussa, G. Molnár, S. Bonhommeau, A. Zwick, S. Mouri, K. Tanaka, J. A. Real, and A. Bousseksou, Phys. Rev. Lett. **94**, 107205 (2005).
[17] N. Ould Moussa, E. Trzop, S. Mouri, S. Zein, G. Molnár, A. B. Gaspar, E. Collet, M. Buron-Le Cointe, J. A. Real, S. Borshch, K. Tanaka, H. Cailleau, and A. Bousseksou, Phys. Rev. B **75**, 054101 (2007).
[18] V. Niel, A. L. Thompson, A. R. Goeta, C. Enachescu, A. Hauser, A. Galet, M. C. Munoz, and J. A. Real, Chem.-Eur. J. **11**, 2047 (2005).
[19] R. J. Glauber, J. Math. Phys. **4**, 294 (1963).
[20] J. Wajenfratz and R. Pick, J. Phys. (Paris), Colloq. **32**, C1 (1971).
[21] J. A. Real, H. Bolvin, A. Bousseksou, A. Dworkin, O. Kahn, F. Varret, and J. Zarembowitch, J. Am. Chem. Soc. **114**, 4650 (1992).
[22] S. Bonhommeau, N. Bréfuel, V. K. Pálfi, G. Molnár, A. Zwick, L. Salmon, J. P. Tuchagues, J. S. Costa, J.-F. Letard, H. Paulsen, and A. Bousseksou, Phys. Chem. Chem. Phys. **7**, 2909 (2005).
[23] A. Hauser, Top. Curr. Chem. **234**, 155 (2004).